Stem Cell Reports
Article

OPEN ACCESS

iPSC-Derived Neural Stem Cells Act via Kinase Inhibition to Exert Neuroprotective Effects in Spinal Muscular Atrophy with Respiratory Distress Type 1

Chiara Simone,[1,2] Monica Nizzardo,[1,2] Federica Rizzo,[1] Margherita Ruggieri,[1] Giulietta Riboldi,[1] Sabrina Salani,[1] Monica Bucchia,[1] Nereo Bresolin,[1] Giacomo P. Comi,[1,3] and Stefania Corti[1,3,*]

[1]Dino Ferrari Centre, Neuroscience Section, Department of Pathophysiology and Transplantation (DEPT), University of Milan, Neurology Unit, IRCCS Foundation Ca' Granda Ospedale Maggiore Policlinico, Via Francesco Sforza 35, 20122 Milan, Italy
[2]Co-first author
[3]Co-senior author
*Correspondence: stefania.corti@unimi.it
http://dx.doi.org/10.1016/j.stemcr.2014.06.004

SUMMARY

Spinal muscular atrophy with respiratory distress type 1 (SMARD1) is a motor neuron disease caused by mutations in the *IGHMBP2* gene, without a cure. Here, we demonstrate that neural stem cells (NSCs) from human-induced pluripotent stem cells (iPSCs) have therapeutic potential in the context of SMARD1. We show that upon transplantation NSCs can appropriately engraft and differentiate in the spinal cord of SMARD1 animals, ameliorating their phenotype, by protecting their endogenous motor neurons. To evaluate the effect of NSCs in the context of human disease, we generated human SMARD1-iPSCs motor neurons that had a significantly reduced survival and axon length. Notably, the coculture with NSCs ameliorate these disease features, an effect attributable to the production of neurotrophic factors and their dual inhibition of GSK-3 and HGK kinases. Our data support the role of iPSC as SMARD1 disease model and their translational potential for therapies in motor neuron disorders.

INTRODUCTION

Spinal muscular atrophy with respiratory distress type 1 (SMARD1, OMIM 604320), also identified as distal spinal muscular atrophy type 1 (DSMA1), is an autosomal recessive motor neuron disorder and the second most frequent form of spinal muscular atrophy after spinal muscular atrophy (SMA) 5q. SMARD1 is characterized by a sudden onset of respiratory distress, usually within the first year of life, with initially distal and later generalized muscle weakness (Eckart et al., 2012). SMARD1 results from mutations in the gene encoding the immunoglobulin microbinding protein 2 (IGHMBP2), which encodes an ATPase/helicase that belongs to the SF1 superfamily (Grohmann et al., 2001; Guenther et al., 2009; Jankowsky et al., 2011). A splice-site mutation in murine *Ighmbp2* causes a neuromuscular disorder similar to the human disease in the *nmd* mouse, representing the animal model of SMARD1 (Cox et al., 1998). How these molecular abnormalities lead to motor neuron degeneration and the disease phenotype in rodents and humans is unknown.

No effective therapies are available for motor neuron diseases, including SMARD1. Neural stem cell (NSC) transplantation represents a possible therapeutic strategy for ameliorating the neurological phenotype by multiple mechanisms, including neuroprotection and cell replacement of different CNS cells (Donnelly et al., 2012).

These positive effects of stem cell transplantation (neural and nonneural cells) have been demonstrated in earlier studies by us and other groups (Corti et al., 2006, 2008, 2009, 2010, 2012; Donnelly et al., 2012). As our work has shown, NSC and neuronal precursor transplantation in animal models improves the phenotype of motor neuron diseases, including SMA, SMARD1, and amyotrophic lateral sclerosis (ALS) (Corti et al., 2006, 2008, 2009, 2010, 2012). In fact, we described that primary murine NSC transplantation can improve the disease phenotype in a SMARD1 mouse model (Corti et al., 2006). Furthermore, a phase I safety trial of direct intraspinal transplantation of NSCs into patients with ALS is in progress, approved by the US Food and Drug Administration (Boulis et al., 2011). Recently, Teng et al. has shown the effectiveness of transplanted NSCs in slowing disease and prolonging survival in ALS mice, rescuing the phenotype completely in 25% of cases (survival increased to more than a year compared to 4 months in untreated animals) (Teng et al., 2012), but 40% of transplanted animals still show only a mild survival improvement. These data represent an unprecedented success in this ALS model because pharmacological/molecular treatments have up to now not produced such remarkably successful therapeutic outcomes. One caveat is represented by the observed variability that might have to do with some variation in the neuroprotective features of transplanted cells and the fact that our understanding of the variables that are critical to therapeutic success

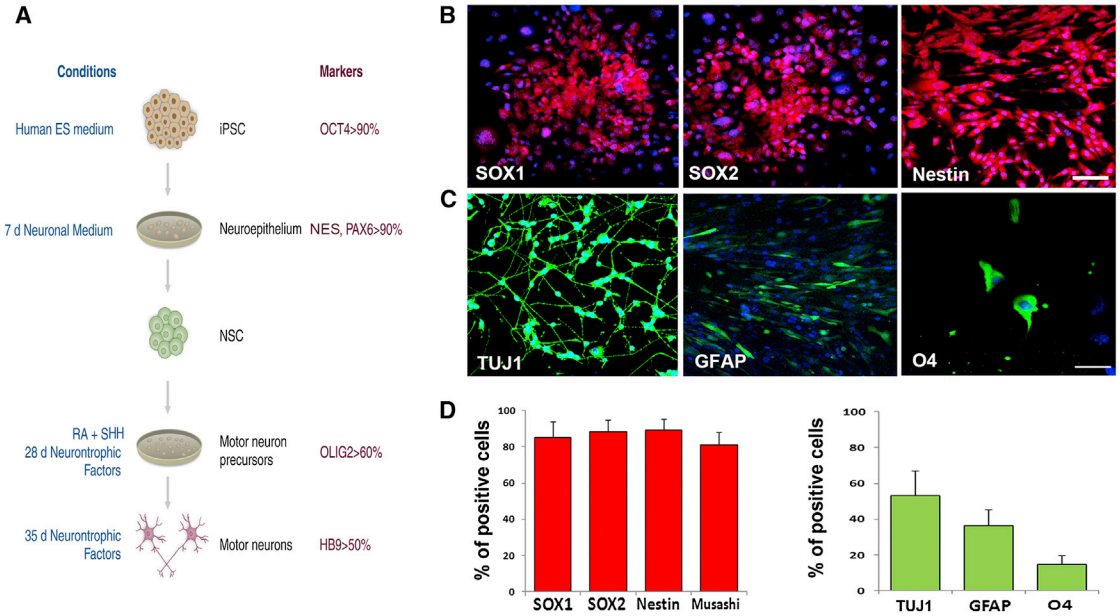

Figure 1. Differentiation of iPSCs into NSCs and Characterization of Their Phenotypic Properties

(A) Scheme for the differentiation of NSCs from iPSCs. The iPSCs were initially undifferentiated and expressed OCT4. After detaching from the plate, the iPSCs formed aggregates that were maintained for 7 days in neural medium. The differentiated cells acquired the features of neuroepithelial (NE) rosettes. The primitive NE cells were positive for PAX6 and nestin. Culturing these cells with RA and SHH generated OLIG2-expressing motor neurons, which were further phenotypically matured in the presence of neurotrophic factors and reduced concentrations of SHH and RA.

(B) iPSC-derived NSCs grown at clonal density in NEP medium generated epithelial-like clones positive for NSC markers such as SOX1, SOX2, and nestin (red). Scale bar, 100 μm.

(C) After in vitro differentiation, NSCs generated the three neuroectodermal lineages, including TUJ1-positive neurons (green), GFAP-positive astrocytes (green), and oligodendrocytes expressing O4 (green), as quantified in (D) (right panel).

(D) Quantification of cells positive for NSC-specific markers (D, left panel). Nuclei were counterstained with DAPI (blue signal). n = 5 independent experiments in triplicate. Scale bar, TUJ1 and GFAP, 100 μm; O4, 50 μm.

remains incomplete. Other persistent limitations include that the source of human NSCs, primary CNS tissue (fetal brain), is limited.

The reprogramming of adult somatic cells into induced pluripotent stem cells (iPSCs) can provide an unlimited source of NSCs for therapeutic use (Ito et al., 2012). Recently, we described that transplantation of a specific NSC population delayed disease progression and extended the life span of ALS mice (Nizzardo et al., 2013).

In the present study, we investigated the therapeutic potential of transplanting human iPSC-derived NSCs into the spinal cord of *nmd* mice, which demonstrated that the engraftment capacity of these cells is associated with an amelioration of the SMARD1 disease phenotype. NSCs are especially remarkable because they can promote cell survival and axonal growth of murine and human SMARD1 motor neurons, which is attributable to the fact that NSCs inhibit both GSK-3 and HGK kinases. This capacity emphasizes that iPSC-derived NSC-mediated therapies hold promising translational potential in motor neuron disorders.

RESULTS

Generation and Characterization of Neural Stem/Precursor Cells from iPSCs

We generated and fully characterized iPSC lines using a nonviral, nonintegrating method (Figure S1 available online). We applied a multistage differentiation protocol previously developed to promote the conversion of human iPSCs into NSCs (Figure 1A) (Corti et al., 2012). These culture conditions resulted in the emergence of rosette conformations typical of neuroepithelial cells. After 7 days, 53.4% ± 6.8% of neural cells expressed Sox1. These cells were then isolated and expanded in media containing epidermal growth factor and fibroblast growth factor (FGF)-2 in adherent conditions. The cells homogeneously expressed NSC marker proteins such as SOX1, SOX2, and nestin (89.3% ± 5.7%) (Figures 1B and 1D) were self-renewing and multipotent and could differentiate into the three major neuroectodermal lineages (Figure 1C). Under differentiation conditions, 53.3% ± 13.8% of the cells generated

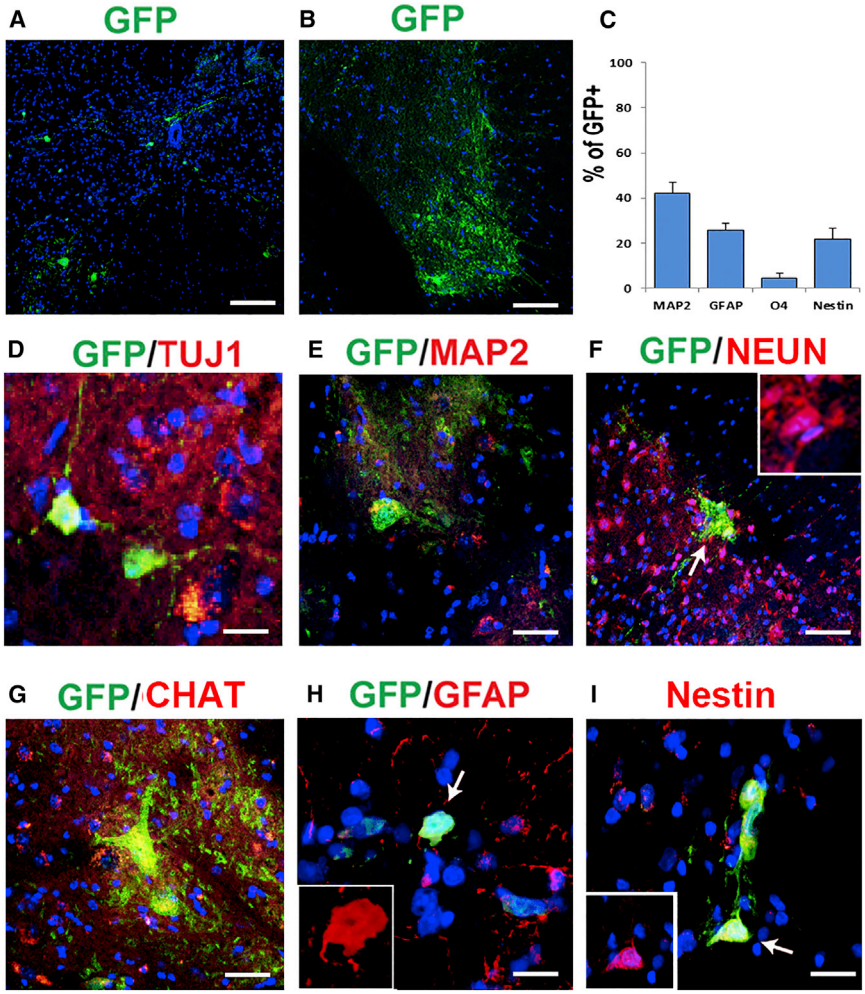

Figure 2. iPSC-Derived NSCs Engraft into the Spinal Cords of *nmd* Mice after Transplantation

(A) After transplantation, the presence of donor GFP$^+$ cells was confirmed in the spinal cord of treated animals. Scale bar, 150 μm.

(B) GFP$^+$ cells were detected in the anterior horns. Scale bar, 75 μm.

(C) Quantification of the phenotype acquired by the donor cells revealed the presence of some undifferentiated cells (nestin), whereas the rest differentiated into neuronal (MAP2) and glial cells (GFAP), with only a minor proportion as oligodendrocytes (O4). The error bars indicate the SD (n = 24 mice per group).

(D–F) Representative images of cells acquiring a neuronal phenotype positive for TUJ1 (D, red), MAP2 (E, red), and NEUN (F, red), as well as for GFP. Scale bars, (D), 75 μm; (E) and (F), 100 μm.

(G) Some cells expressed CHAT (red), suggesting a differentiation of cholinergic neurons. Scale bar, 100 μm.

(H and I) Donor cells also differentiated into astrocytes positive for GFAP (H, red) or maintained an undifferentiated phenotype expressing nestin (I, red). Nuclei were counterstained with DAPI (blue signal). Scale bars, (H) 100 μm; (I) 75 μm.

TUJ1-positive neurons (Figure 1C) with extended neuronal processes. We then tested whether these NSCs could give rise to clinically relevant neuronal subtypes such as spinal cord motor neurons. Following the protocols developed for human pluripotent stem cells (Hu and Zhang, 2009; Corti et al., 2012), we exposed the NSCs to sonic hedgehog (SHH) and retinoic acid (RA) in the presence of neurotrophins (Figure 1A). Quantification revealed that the number of choline acetyltransferase (CHAT)-positive neurons was 37.8% ± 6.9%. In addition to neuronal antigens (MAP2), these cells also expressed other specific motor neuronal markers (ISLET-1, HB9) (Figure S2).

Transplanted iPSC-Derived NSCs Engraft into the SMARD1 Spinal Cord and Differentiate into the Three Major Neuroectodermal Lineages

To investigate the therapeutic potential of wild-type (WT) iPSC-derived NSCs, we injected green fluorescent protein (GFP)-labeled NSCs (10,000 cells × two horns at the cervical and lumbar levels) into SMARD1 mice at 1 day of age (postnatal day 1) according to a previously described transplantation protocol. Control mice received only vehicle or fibroblasts cells. Dye injection, used as a control, showed the distribution of the injected solution in the spinal cord and the absence of any damage (Figure S3). The transplanted mice were analyzed at the end stage of the disease. Transplanted cells were detected in the gray matter of the treated spinal cord (Figures 2A and 2B). Unbiased stereological quantification with optical dissectors and random sampling of GFP-engrafted cells demonstrated that an average of 8,795 ± 526 donor cells were present (Table 1).

To analyze the phenotype of engrafted cells, we performed confocal immunohistochemical analysis of neuroectodermal antigens. The human donor cells displayed various complex neuronal and glial morphologies expressing the neuronal marker proteins β-III-tubulin (Figure 2D) and NEUN (Figure 2F), the astrocytic marker glial fibrillary acidic protein (GFAP; Figure 2H), or the progenitor cell marker nestin (Figure 2I). The predominant phenotype of

Table 1. Stereological Quantification of Donor Cells in *nmd* Spinal Cord after Transplantation

No of animal analyzed	24
Total cell counts	8,795 ± 526

transplanted cells was neuronal, as demonstrated by double-positive staining for the neuronal-specific antigen MAP2 and GFP (41.9% ± 5.2%) (Figures 2C and 2E). Immunohistochemical detection of the combined presence of glial antigens (glial fibrillary acidic protein and O4) and GFP demonstrated that astrocytes comprised 25.6% ± 3.1% of the cells, whereas 4.4% ± 2.4% were oligodendrocytes (Figure 2C). In addition, 21.6% ± 5.1% of GFP donor cells maintained the features of NSC/progenitor cells and expressed both nestin and GFP (Figure 2C).

We also evaluated whether engrafted NSCs can acquire a motor neuronal phenotype. A fraction of the transplanted cells presented motor neuronal features, as suggested by their morphology and reactivity for motor-neuron-specific markers, including CHAT (Figure 2G). Unbiased stereological quantification demonstrated that the number of CHAT-GFP cells was 4.1% ± 0.3% cells per spinal cord. No adverse effects were observed after iPSC-derived NSC transplantation.

Transplantation of iPSC-Derived NSCs Improves the Neuromuscular Phenotype and Increases Survival of SMARD1 Mice

We evaluated whether transplantation of WT iPSC-derived NSCs could ameliorate the phenotype and extend survival in *nmd* mice. Functional recovery was assessed in all animal groups by blind assessment of their overall appearance, weight, neuromuscular function (rotarod test), and survival after transplantation (Figure 3). The first clinical symptoms in *nmd* mice presented in the second postnatal week. The mice then rapidly developed muscle weakness starting in the hind limbs, which were dorsally contracted, causing impaired locomotor activity. The limited limb extension made standing on all four limbs impossible. Homozygotes clenched their hind limbs when picked up by the tail and could not grasp a cage cover when held against it. As the disease progressed, the weakness was generalized to involve the forelimbs. At 3 weeks, in transplanted *nmd* mice, the hind limb muscles were ameliorated in comparison to their *nmd* littermates, who presented muscle wasting and marked contracture of the hind limbs (Figure 3A). Mutant mice were severely paralyzed by the age of 5 weeks. At the age of 5 weeks, all *nmd* mice failed the rotarod test and could not remain on the accelerating wheel for longer than a few seconds ($p < 0.0001$ versus control siblings) (Figure 3B).

By contrast, transplanted *nmd* mice at 3 weeks of age did not present a typical hind limb posture and could still perform the rotarod test at 5 weeks of age ($p < 0.0001$ versus untreated), although they exhibited a decrease in performance when compared with their wild-type (WT) siblings. At each time point, the performance of the transplanted *nmd* mice was significantly superior to the untreated animals ($p < 0.0001$ versus untreated *nmd* mice, until 8 weeks) (Figure 3B). The growth rates of the transplanted and untransplanted *nmd* mice, as measured by mean body weight, were almost indistinguishable from that of their control littermates from birth up to 1 week of age; however, starting from 2 weeks of age, the *nmd* mice presented a reduced mean body weight compared with their control siblings. By contrast, transplanted *nmd* mice displayed an intermediate growth rate significantly different from that of untreated *nmd* mice and controls at 8 weeks (transplanted: 16.9 ± 1.9 g versus vehicle-treated: 12.8 ± 1.4 versus fibroblast-treated 11.9 ± 1.7; $p < 0.0001$, $n = 24$ per group) (Figure 3C). The transplanted *nmd* mice also had significantly increased mean lifespans compared to sib-matched vehicle and fibroblasts-treated *nmd* mice; thus, the effect was specific (treated 92.3 ± 27.8 versus vehicle 69.6 ± 27.3; $p = 0.006$; $n = 24$; $\chi^2 = 7.3$; versus fibroblasts treated: 67.2 ± 28.2 $p = 0.004$; $n = 24$; $\chi^2 = 8.2$) (Figure 3D).

Donor Cells Provide Neuroprotection to Endogenous Motor Neurons and Their Muscle Connections

To analyze the factors underlying the improved motor behavior and survival in transplanted *nmd* mice, we investigated spinal cord motor neurons and ventral spinal nerve roots from a quantitative perspective (Figure 4). Relative to WT littermates, a severe loss of spinal motor neurons was detected in vehicle-treated *nmd* mice. By contrast, in transplanted *nmd* mice, we detected a significant protection of motor neurons in the lumbar spinal cord, with a 65% preservation of motor neurons at 6 weeks with respect to 44% in untreated mice (transplanted versus nontransplanted mice $p < 0.0001$) (Figure 4A). At the end stage of the disease, the number of motor neurons in untreated animals was reduced to 25% of that observed in WT, whereas transplanted *nmd* animals retained 42% (treated versus untreated *nmd*, $p < 0.0001$) (Figure 4B). Prominent neuronal loss was observed in 6-week-old *nmd* mice, as evidenced by a significant reduction in the diameter of the L4–L5 ventral nerve roots. Similar reductions were detected in all lumbar ventral roots analyzed. By contrast, only a limited reduction was detected in the diameter of ventral roots of age-matched transplanted mice (Figures 4C and 4D). The transplanted animals also presented a partial preservation of large axon density (Figures 4E and 4F). These data suggest that neuroprotection is a key factor in the beneficial effect of NSC transplantation in *nmd* mice.

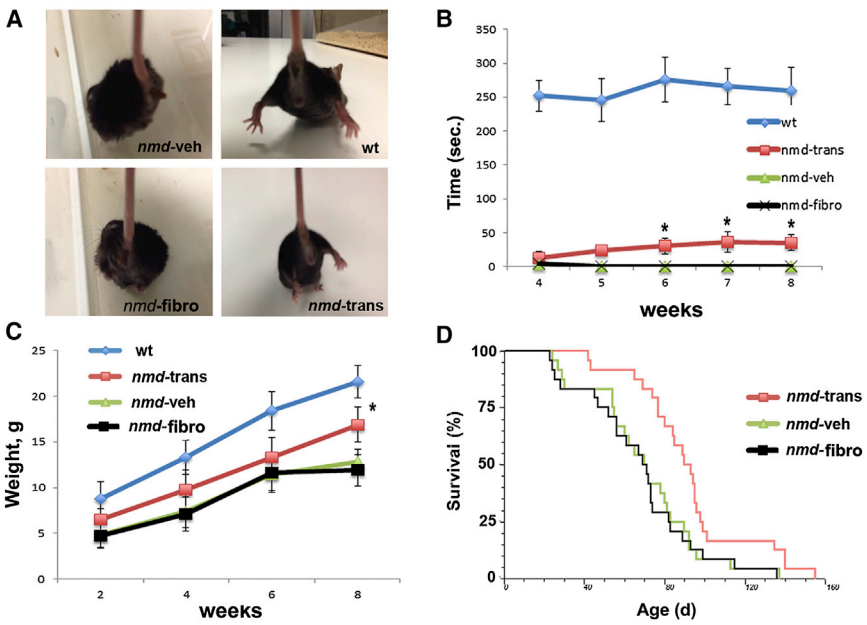

Figure 3. NSC Transplantation Improves Neuromuscular Function and Survival in *nmd* Mice

(A) Representative pictures of transplanted *nmd* mice (*nmd*-trans) showing their greater capacity to open and extend their lower limbs in comparison to vehicle-treated (*nmd*-veh) and fibroblasts-treated (*nmd*-fibro) animals, with features similar to wild-type (WT).

(B) The time that transplanted mice could remain on the rotarod treadmill was increased relative to *nmd*-veh mice and *nmd*-fibro at 8 weeks of age (n = 24 per group; *p < 0.0001). Error bars show the SDs.

(C) The mean body weight of *nmd*-trans mice was increased relative to *nmd*-veh mice and *nmd*-fibro (at 8 weeks; n = 24 per group; *p < 0.0001).

(D) Kaplan-Meier survival curves of *nmd*-trans and *nmd*-veh mice; *nmd*-trans mice (n = 24 per group) survived significantly longer than *nmd*-veh (p = 0.006) and *nmd*-fibro mice (p = 0.004).

WT iPSC-Derived NSCs Produce Neuroprotective Factors and Positively Influence SMARD1 Murine Motor Neurons

The improvement in *nmd* mice after transplantation led to our investigation of possible mechanisms, in which we assessed whether or not WT iPSC-derived NSCs produce neuroprotective factors that affect SMARD1 murine motor neurons (Figures 5A–5D). The results indicated that NSCs do indeed produce such factors, including glial cell-derived neurotrophic factor (GDNF), brain-derived neurotrophic factor (BDNF), transforming growth factor-α (TGF-α), and neurotrophin-3 (NT3) (Figures 5A–5D).

To identify donor NSC effects on SMARD1 pathogenesis, we used a coculture system containing a bottom layer of primary motor neurons from *nmd* mice and a top layer of human WT NSCs seeded onto a microporous membrane, which permits the diffusion of soluble factors only into the lower compartment (Figure 5E). Typical images of the axon/growth cone are shown in Figures 5F and 5G. Alone, SMARD1 mouse primary motor neurons had much shorter axons compared to wild-type motor neurons ($p < 0.00001$) (Figure 5H). However, coculture of the SMARD1 motor neurons in the presence of human NSCs resulted in an increased axon length (Figure 5H). Furthermore, the *nmd* mice had significantly smaller motor neuron growth cones compared to wild-type ($p < 0.00001$), and their growth cone size increased following NSC coculture ($p < 0.00001$) (Figure 5I). These results suggested that neurotrophin expression could enhance axon length, which we tested by neutralizing individual cytokines or combinations of cytokines with antibodies added to the culture media. The result was a significantly reduced axon length for *nmd* mouse motor neurons following neutralization of GDNF, BDNF, and NT3 ($p < 0.01$) (Figure 5J).

Then, we investigated the effects of NSCs on *nmd* neuronal survival. *Nmd* motor neurons in standard motor neuronal medium do not present a reduction in cell survival; however, in a neurotoxic environment, which was provided by lipopolysaccharide-activated microglial-conditioned media, they present a reduction in cell survival respect to wild-type cells (Figures 5K and 5L). In this experimental setting, we demonstrated that exposure to NSCs significantly promoted *nmd* mouse motor neuron survival ($p < 0.001$ versus untreated cells) in an inflammatory/toxic environment.

WT NSCs Protect Vulnerable iPSC Spinal Motor Neurons Derived from SMARD1 Patients

Our next question was whether or not WT iPSC-derived NSCs protect human SMARD1 iPSC-derived motor neurons against degeneration induced by loss of IGHMBP2. For this purpose, we reprogrammed fibroblasts of SMARD1 patients and healthy individuals into iPSCs (Table 2) and differentiated them in motor neurons. The direct monitoring of the phenotype was obtained with a transduction of a lenti-*Hb9*::eGFP construct (Marchetto et al., 2008). In addition, we evaluated the effect of WT NSCs on SMARD1 motor neurons (Figure 6A). The human motor neurons

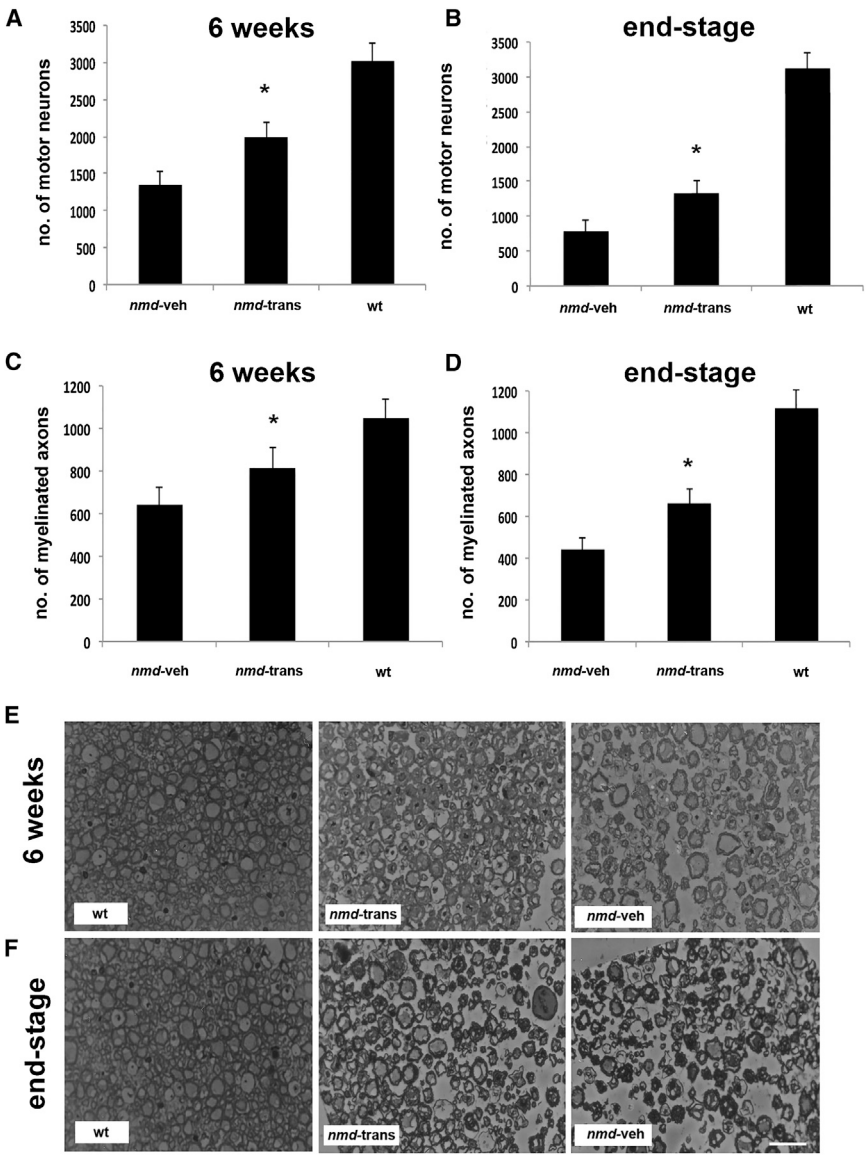

Figure 4. NSC Transplantation Increases Motor Neuron and Axon Number

(A and B) Motor neuronal count in the lumbar spinal cord of transplanted (*nmd*-trans), vehicle-treated (*nmd*-veh), and wild-type (WT) mice (data represent the mean ± SD) at 6 weeks of age (A) and at the end stage of the disease (B) (n = 6 per group per time point).

(C and D) Quantification of axons in the L4 anterior roots in WT, *nmd*-veh, and *nmd*-trans (the data represent the mean ± SD) at 6 weeks of age (C) and at the end stage of the disease (D) (n = 6 per group per time point). These data demonstrate a significant increase in motor neuron and axon counts after transplantation compared to *nmd*-veh mice (*$p < 0.0001$).

(E and F) Representative cross-section pictures of L4 ventral roots of spinal cord lumbar segment from WT mice, *nmd*-trans mice, and *nmd*-veh mice at 6 weeks of age (E) and at the end stage of the disease (F). Scale bar, 50 μm.

extended processes and expressed HB9 and CHAT (Figure 6B). For further evaluation, we examined some motor neuron features that are likely relevant to SMARD1 pathogenesis, including cell survival, axonal elongation, and growth cone formation. Although at 5 weeks we observed no significant reduction in cell number and axonal length (Figures 6C–6E), at 8 weeks SMARD1 iPSC-derived motor neurons had a significantly reduced cell number and axon length compared to those from WT iPSCs ($p < 0.001$), indicating an apparent cell autonomous degeneration in vitro of SMARD1 motor neurons in long-term culture, rather than a developmental defect (Figures 6F–6H).

Addition of human NSCs (hNSCs), however, in coculture with SMARD1 motor neurons protected the neurons, which had improved survival at 8 weeks of culture ($p < 0.001$, ANOVA) (Figure 6F). The SMARD1 motor neurons that were cocultured with NSC also had increased neurite lengths compared to untreated neurons ($p < 0.001$, Kolmogorov-Smirnov test) (Figure 6G). Thus, NSCs can protect human motor neurons from SMARD1-induced degeneration.

We hypothesized that upregulation of neurotrophin expression might be involved in this amelioration, as was the case in murine motor neurons, so we again neutralized the relevant cytokines by adding neutralizing antibodies to the media. Neutralizing GDNF and BDNF, which we selected based on the murine findings, resulted in significantly decreased axon length for SMARD1 motor neurons ($p < 0.01$) (Figure 6H).

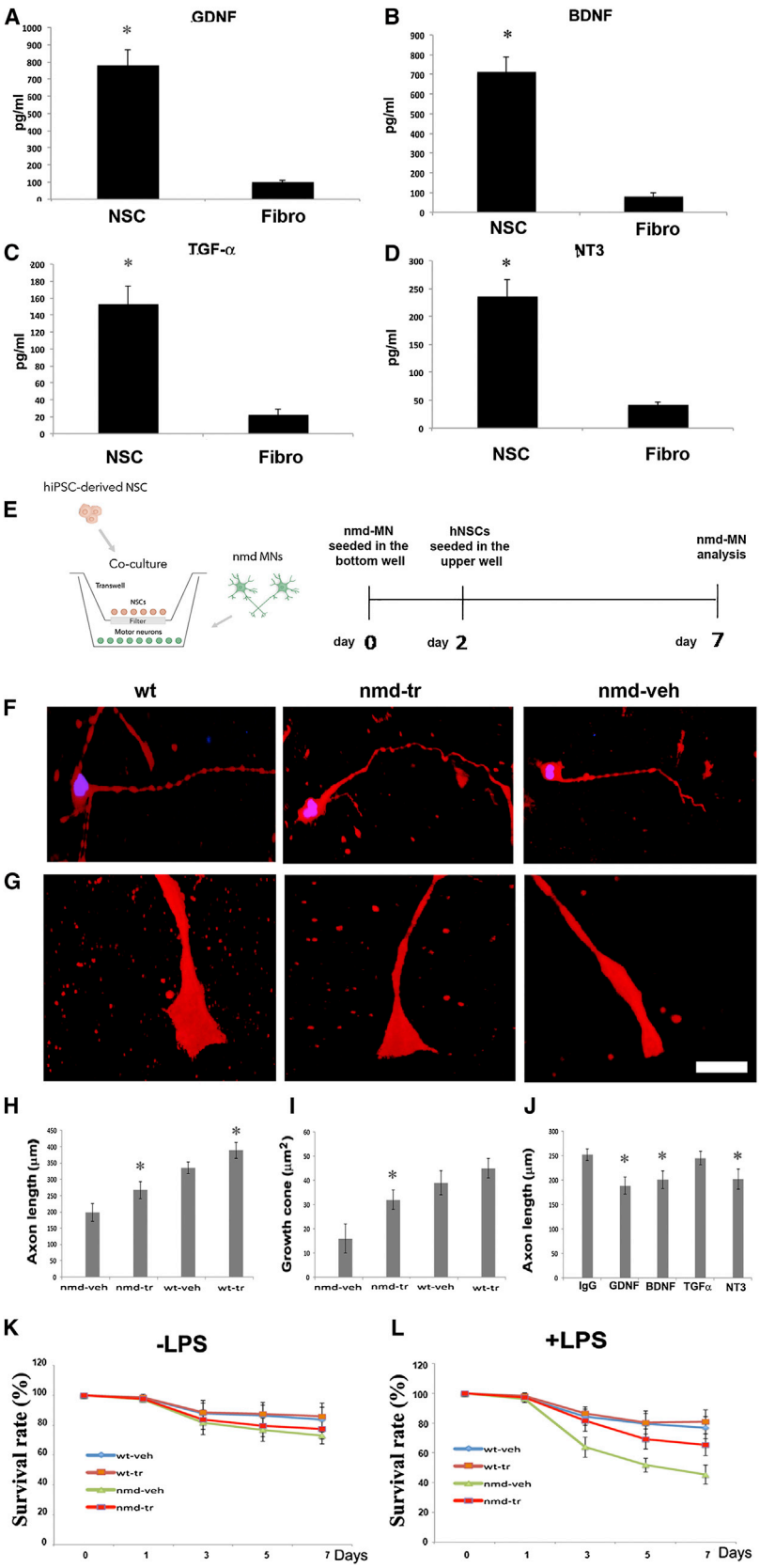

Figure 5. NSCs Produce Neurotrophins and Protect Motor Neurons of *nmd* Mice

(A–D) The amounts of (A) GDNF, (B) BDNF, (C) TGF-α, and (D) NT3 secreted by NSCs were determined by ELISA, which revealed a significant production of these neuroprotective substances in comparison to fibroblasts *p < 0.00001, two-tailed Student's t test. Mean ± SD, n = 12 independent experiments for each cytokine.

(E) Schematic diagram of the coculture of human NSCs and *nmd* motor neurons.

(F) Representative images of neurite outgrowth. Cells were stained with phospho-tau protein (red signal). Nuclei were counterstained with DAPI (blue signal).

(G) High-power magnification of NF-stained (red) axonal growth cones in cultured motor neurons.

(H and I) Average length of axons (H) and growth cone area of motor neurons (I) from *nmd* mice, in coculture with human NSCs. Motor neurons from SMA mice cocultured with human NSCs (treated, tr) exhibited an increase in axon length and size of growth cone with respect to *nmd* mouse motor neurons not cocultured with human NSCs (vehicle, veh) (*p < 0.00001, two-tailed Student's t test; mean ± SD, n = 4 independent experiments for each condition).

(J) The average axonal length of cocultured *nmd* mouse motor neurons was reduced after cytokine neutralization of cytokine production by human NSCs in the case of GDNF, BDNF, and NT3 (*p < 0.01, two-tailed Student's t test; mean ± SD, n = 4 independent experiments for each condition).

(K and L) Quantification of the number of SMI32-positive *nmd* murine motor neurons in the presence of human NSC and microglial-conditioned media with (K) and without (L) LPS. The number of *nmd* mouse motor neurons in cultures with microglia^{+} LPS was reduced but was increased in coculture with human NSC (*p < 0.001, ANOVA, mean ± SD, n = 4 independent experiments for each condition). Scale bars, (F) 75 μm; (G) 5 μm.

Table 2. Characteristics of Human Fibroblast-Derived Induced Pluripotent Stem Cell SMARD1 Lines and Their Controls

iPSC Line	Diagnosis	Mutations IGHMBP2	Sex	Age	Reprogramming Strategy	Reference
SMARD 1.1	SMARD I	c.2125C > Tp.709Q > X	Female	3	nonviral 6 factors: OSKM+LN	this report
SMARD 1.2	SMARD I	c.2125C > Tp.709Q > X	Female	3	nonviral 6 factors: OSKM+LN	this report
SMARD 1.3	SMARD I	c.2125C > Tp.709Q > X	Female	3	nonviral 6 factors: OSKM+LN	this report
SMARD 2.1	SMARD I	c.121 delC/c.439C > T p.Gln41ArgfsX48/p.Arg147X	Female	2	nonviral 6 factors: OSKM+LN	this report
SMARD 2.2	SMARD I	c.121 delC/c.439C > T p.Gln41ArgfsX48/p.Arg147X	Female	2	nonviral 6 factors: OSKM+LN	this report
SMARD 2.3	SMARD I	c.121 delC/c.439C > T p.Gln41ArgfsX48/p.Arg147X	Female	2	nonviral 6 factors: OSKM+LN	this report
19.9	healthy donor	—	Male	newborn	nonviral 6 factors: OSKM+LN	Yu et al., 2009
CTR AC 1.1	healthy donor	—	Female	24	nonviral 6 factors: OSKM+LN	this report
CTR AC 1.2	healthy donor	—	Female	24	nonviral 6 factors: OSKM+LN	this report
CTR AC 13	healthy donor	—	Female	24	nonviral 6 factors: OSKM+LN	this report

NSC Coculture Promotes Kinase Inhibition in Human Motor Neurons

Because it has been described that the GSK-3 and HGK kinases pathways can regulate motor neuronal survival of ALS and wild-type motor neurons (Yang et al., 2013), we sought to examine if NSCs could protect human SMARD1 motor neurons from death caused by inactivation of PI3K/AKT and HGK kinases.

Growth factors such as GDNF are reported to be activators of the AKT/PI3K pathway that in turn inhibits GSK3β activity (Zuo et al., 2013). Furthermore, PI3K/Akt activity is decreased in motor neurons of both sporadic and familial ALS patients, as well as in mutant *SOD1* mice, whereas activation of PI3K/Akt or inhibition of GSK3β can increase ALS motor neuron survival (Yang et al., 2013). To identify molecular targets that might be acted on by NSCs to protect SMARD1 motor neurons, we carried out studies employing a Phospho-Kinase Antibody Assay to examine the site-specific phosphorylation of GSK3β in the presence or absence of NSCs in motor neuron cocultures. In NSC-treated SMARD1 motor neurons, levels of GSK-3PSe9 phosphorylation were strongly elevated in a dose-dependent manner in coculture conditions, as demonstrated by immunocytochemistry and western blot ($p < 0.01$) (Figures 7A–7C), indicating that GSK-3P was inhibited.

NSCs can act on a biologically and pharmacologically meaningful target, GSK-3, so we tested further commercially available GSK-3 inhibitors in our survival assay. Of these, GSK-3 inhibitors VIII and XIII (Yang et al., 2013) produced a consistent survival improvement but one that was reduced compared to the effect of NSCs (Figure 7D). As an additional step, we compared NSCs and these two GSK-3 inhibitors (10 μM) for their ability to protect motor neurons from death resulting from PI3K/AKT inactivation. Coincubation of NSCs with the PI3K inhibitor LY294002 (10 μM) attenuated the motor neuron death that LY294002 alone induced (Figure 7D). We found that the VIII and XIII inhibitors conferred some protection on SMARD1 motor neurons but produced only a small increase in motor neuron survival respect to NSCs. Similar results were obtained using the more potent and selective PI3K inhibitor PI-103 (1 μM) (Figure 7D). Overall, these findings indicated that inhibiting GSK-3 might assist in promoting survival, but the possibility remained that the comparatively superior effect of NSCs might arise from additional molecular events.

Thus, we assessed the HG kinase pathway and showed that NSC blocks the JNK/c-JUN-mediated cell death signaling cascade in SMARD1 motor neurons that are under the control of HG kinase. HG is a kinase involved in the phospho-c-JUN-mediated neuronal cell death pathway, and inhibition of this kinase prevents activation of apoptosis. JNK is part of a central stress signaling pathway implicated in neuronal plasticity, regeneration, and cell death of neuronal and nonneuronal cells (Herdegen et al., 1997).

As shown in Figure S4, exposure of SMARD1 motor neurons to NSCs blocks phosphorylation and therefore activation of c-JUN, JNK, MKK4, and TAK1 (Figure S4). Therefore, in the coculture system, NSCs may exert neuroprotective effects by blocking activation of the proapoptotic JNK, MKK4, and TAK1 signaling cascade.

Our results support the hypothesis that NSC treatment inhibits activation of GSK-3 and HGK kinases in our motor

neuron cultures and are consistent with the idea that this inhibition may be a significant therapeutic target for SMARD1.

DISCUSSION

Increasing preclinical evidence suggests that NSC transplantation can exert a therapeutic effect on motor neuron disease phenotypes (Donnelly et al., 2012). This positive effect is likely related to multiple mechanisms including not only replacement of different CNS cell populations but also neuroprotection of host motor neurons by different factors produced by donor cells (Boulis et al., 2011). Previously, we reported that primary murine NSC transplantation can improve the disease phenotype in a SMARD1 mouse model (Corti et al., 2006). These data demonstrated the therapeutic potential of NSC transplantation for this disease.

In the present study, we demonstrated that transplanted human iPSC-derived NSCs can engraft into the SMARD1 spinal cord, also in the anterior horns, the areas of active degeneration, after which they differentiate into the three major neuroectodermal lineages and generate motor-neuron-like cells, even if in a small proportion. Transplantation of iPSC-derived NSCs significantly improved the neurological phenotype and survival of *nmd* mice. Indeed, this transplantation significantly correlated with a reduced pathology of the spinal cord and protection of endogenous motor neurons. These results build upon the findings from our previous work in regards to translational possibilities: pluripotent cell sources, particularly iPSCs, are much more readily available and accessible than CNS primary-derived NSCs.

With these results, we provide evidence that the transplantation of iPSC-derived NSCs could have a beneficial role in modifying the course of SMARD1. Regarding the translational safety of iPSC-derived cells, one major finding of this study is that adverse events such as tumorigenesis or abnormal growth were not observed, even if our observational time is limited. Although NSC transplantation was not sufficient to fully rescue the *nmd* phenotype, the behavioral improvements and enhanced survival were significant. The neurological phenotypic improvement correlated with a significant modification in spinal cord pathology, and the motor neuron count in NSC-transplanted relative to vehicle-treated and fibroblasts-treated mice confirmed a significant reduction in neural cell degeneration.

We observed the generation of a low proportion of donor-derived motor neurons, as evaluated by immunopathological characterization, which were correctly located in the anterior horns. In addition, we detected an increased number of endogenous motor neurons as well as myelinated axons in iPSC-transplanted *nmd* mice compared with vehicle-treated controls. Overall, the functional improvement in the SMARD1 mouse models was supported by the results of our neuromuscular function tests and by the improved survival of transplanted mice. NSC transplantation increased survival by 30% compared with the vehicle-treated group. The extended survival time resulting from stem cell transplantation, although limited, is a significant finding. Similarly, the neuromuscular function test results in this study must be considered in the context of decreased disease severity; treated animals could perform the rotarod task, even if with lower performance respect to the wild-type, whereas untreated animals would never be able to execute the task. Therefore, although the amelioration was not complete, it was relatively substantial.

In addition, human iPSC-derived NSCs produce neurotrophic factors that may be neuroprotective of murine and human motor neurons by paracrine signaling, as our coculture results suggest. This neurotrophic benefit of NSCs indicates that they can lessen some of the effects of SMARD1 pathogenesis. Particularly promising is the finding that NSCs exert this protection in motor neurons derived from reprogrammed SMARD1 fibroblasts. We also showed that iPSCs from SMARD1 patients are a suitable model for evaluating cellular features of motor neuron disease degeneration. Overall, NSC coculture improved motor neuron survival, increased neurite length, and boosted growth cone size of SMARD1 iPSC-derived motor neurons. Our mechanistic studies of NSC protective effects of human SMARD1 motor neurons showed that NSC coculture increased GSK3β phosphorylation, which would be expected to elicit decreased kinase activity, a feature associated with motor neuron survival (Yang et al., 2013). In keeping with this finding, our results also demonstrated that NSC coculture inhibits the JNK/c-JUN-mediated cell death signaling cascade in motor neurons that HGK kinase controls. Overall, these findings indicate that NSC treatment inhibits GSK-3 and HGK kinase activation in our motor neuron cultures and suggest an important therapeutic target for SMARD1.

In conclusion, this report provides evidence that NSCs derived from pluripotent cells are a potentially useful therapeutic tool to ameliorate SMARD1 disease phenotype. Combining cell transplantation treatment with drug or gene therapy might further increase the therapeutic efficacy to a clinically significant level for SMARD1 and other motor neuron diseases.

EXPERIMENTAL PROCEDURES

Generation of iPSCs

Reprogramming of human skin fibroblasts was executed as previously described (Corti et al., 2012) with oriP/EBNA1-based episomal vectors encoding the human genes *OCT4*, *SOX2*,

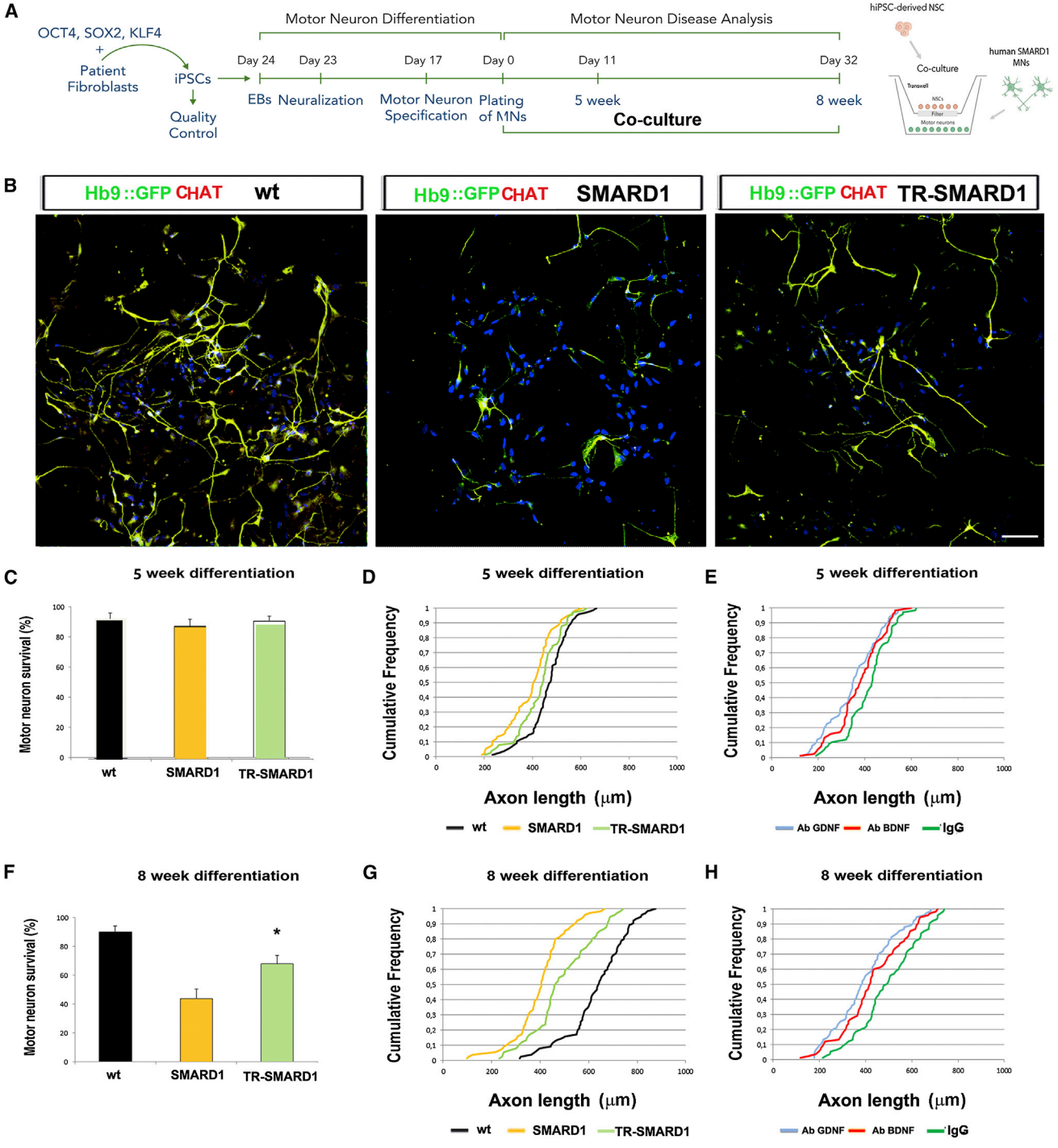

Figure 6. NSCs Protect Human Spinal Motor Neurons in Culture from SMARD1 Degeneration

(A) Schematic diagram of experimental design: motor neuron differentiation and coculture of SMARD1 cells with wild-type human NSCs. (B) Representative images of SMARD1 motor neurons in culture: compared to wild-type (left panel), the number of SMARD1 motor neurons is significantly decreased in long-term culture without NSCs (middle panel) (n = 5 independent experiments for each condition). The coculture with NSCs increased the number of SMARD1 motor neuron (right panel). Motor neurons were stained with Hb9::GFP (green) and CHAT (red) and nuclei were counterstained with DAPI (blue signal). Merged images are presented. Scale bar, 75 μm.

(legend continued on next page)

NANOG, *LIN28*, *c-MYC*, and *KLF4*. After nucleofection, fibroblasts were seeded onto 3 × 10 cm dishes covered with Matrigel (BD Biosciences) in fibroblast culture medium, which was changed every other day. At 4 days after transfection, we substituted the fibroblast culture medium with human embryonic stem cell culture medium (mTeSR, STEMCELL Technologies) for 8–10 days. At day 18 after transfection, it was possible to recognize colonies with an iPSC-like morphology. We then isolated the iPSC colonies that were morphologically more similar to embryonic stem cells for further analysis and expansion, as previously described (Corti et al., 2012).

Differentiation of iPSCs into NSCs

We differentiated iPSCs into neuroepithelial cells using a previously described differentiation protocol (Corti et al., 2012). iPSCs were seeded in neuronal medium based on Dulbecco's modified Eagle's medium/F12 (Gibco, Invitrogen), supplemented with MEM nonessential amino acids solution, N2, and heparin (2 μg/ml; Sigma-Aldrich), thus promoting neuroepithelial differentiation.

For cell expansion and clonal culture, NSCs were plated in growth medium (NEP medium) containing FGF with or without epidermal growth factor, as previously reported (Corti et al., 2008).

Immunocytochemistry of iPSCs and Their Derivatives

Cells were fixed in 4% paraformaldehyde for 10 min, permeabilized with 0.5% Tween 20 in PBS, and exposed to 0.1% Tween 20 with 10% horse serum. We incubated the cells with primary antibodies overnight and with secondary antibodies for 1 hr (Alexa Fluor, Invitrogen). We employed the following primary antibodies: SSEA-3 (1:100, Chemicon), SSEA-4 (1:500, Chemicon), TRA1-60 (1:500, Chemicon), TRA1-81 (1:500, Chemicon), nestin (1:200, Millipore), SOX1 (1:1000, R&D Systems), SOX2 (1:1000, Millipore), TUJ1 (1:200, Millipore), GFAP (1:300, Sigma), Islet1/2 (1:200, Millipore), HB9 (1:200 Millipore), CHAT (1:200, Millipore), MAP2 (mouse monoclonal, 1:100; Sigma), O4 (10–20 μg/ml, Millipore), and Musashi (1:200, Novus Biologicals). The *Hb9*::GFP gene reporter was used to identify motor neuron cells, as described previously (Marchetto et al., 2008). For all imaging, we used a confocal LEICA LCS2 microscope.

Animal Models

The *nmd* mouse (B6.BKS *Ighmbp2nmd-2J/J*) possesses a homozygous mutation in the *Ighmbp2* gene. Heterozygous mice were bred to generate mice homozygous for the mutation. Homozygous *nmd* mutant mice and WT littermates were employed for the experiments and analyses. The genotypes of the mice were confirmed using a PCR-based assay with genomic DNA from tail biopsies as described previously (Cox et al., 1998). All transgenic animals were purchased from Jackson Laboratory. All animal experiments were approved by the University of Milan and Italian Ministry of Health review boards, in compliance with US National Institutes of Health Guidelines (Corti et al., 2006).

Neural Stem Cell Transplantation

Before cell transplantation, the donor cells were genetically engineered to express *GFP* under a cytomegalovirus promoter (Corti et al., 2012). The cells were harvested and prepared for transplantation as described previously (Corti et al., 2012). The graft recipients were 1-day-old *nmd* mice. As previously described, cells were transplanted into the spinal cords of animals after cryoanesthesia (Corti et al., 2009, 2010, 2012). An injection micropipette (100 μm tip diameter) was inserted into the anterior horns. A slow infusion of 2 μl of cell suspension (10,000 cells/μl × two horns) was injected into the C4–C5 and L1–L2 regions of the recipients' spinal cords. After injection, the needle was slowly removed. All of the transplanted mice survived after the injection without any observed side effects. As controls, *nmd* mice received vehicle or human fibroblasts only using the same surgical procedure (Corti et al., 2009, 2010, 2012). The experimental group included 24 mice (12 males), as did the vehicle control group (24 mice; 12 males). The animals were evaluated by a blinded examiner for weight, rotarod performance, survival record, and histological evaluation of donor cell phenotype until the end stage. The immunosuppressor FK506 was administered intraperitoneally at 1.0 mg/kg to all animals in all groups for the entire length of the experiment.

The study was designed so that littermates were distributed equally among the transplanted and untransplanted groups. Separate groups of animals (each composed of six mice per time point per condition) were sacrificed for histological analysis, quantification of motor neurons and axons, and muscle analysis.

Neuromuscular Evaluation and Survival

All groups of *nmd* mice were monitored daily after transplantation or vehicle injection for phenotypic hallmarks of disease. The investigators that executed the functional assessment were blind to the treatment. Body weight was recorded, and motor function

(C–E) At 5 weeks, no difference was detected in number of SMARD1 motor neurons with respect to wild-type as well as in their axonal lengths in basal conditions (D) and after exposure to antibodies neutralizing neurotrophins (E). ANOVA (n = 5 independent experiments for each condition).

(F) Treatment of the cultures with NSCs was protective of motor neurons in long-term culture, increasing their survival respect to untreated cells (8 weeks, *$p < 0.001$, ANOVA, n = 5 independent experiments for each condition).

(G) At 8 weeks, untreated SMARD1 motor neurons had shorter axons than wild-type cells. SMARD1 motor neurons cocultured with NSCs had longer axons than untreated SMARD1 motor neurons ($p < 0.001$, Kolmogorov-Smirnov test, n = 5 independent experiments for each condition).

(H) Relevant cytokines were neutralized by antibody addition to the motor neuron culture media; neutralizing GDNF and BDNF significantly reduced axon length of SMARD1 motor neurons respect to control immunoglobulin G (IgG). These growth factors were selected based on murine data ($p < 0.01$, n = 5 independent experiments for each condition). These experiments were performed with iPSC lines of two SMARD1 patients and WT subjects (three clones for each subject).

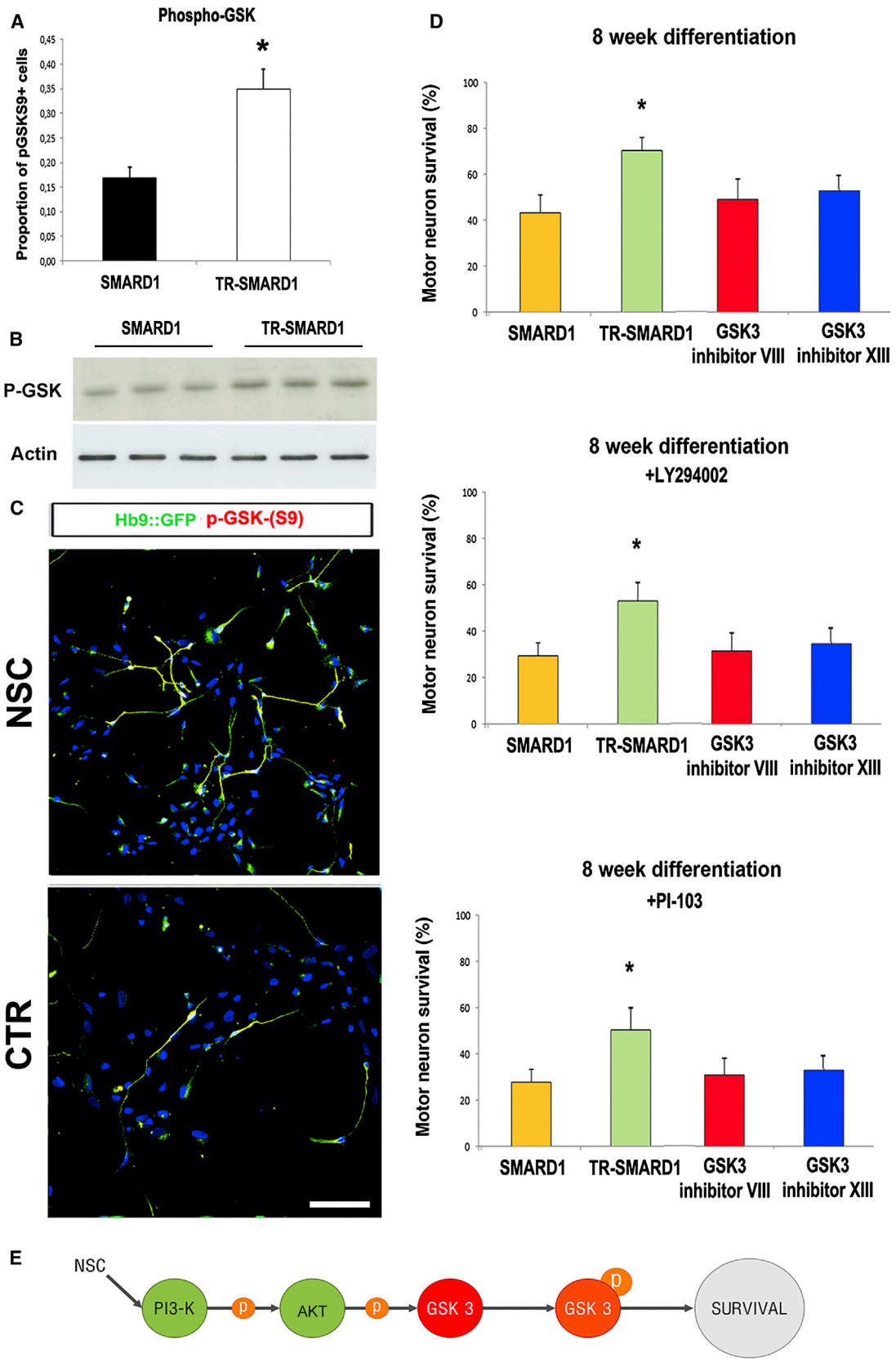

(legend on next page)

was tested weekly with an accelerating rotarod device (4–40 rpm; Rota-Rod 7650; Ugo Basile). We recorded the length of time that each mouse remained on the rotarod. Mortality was scored as the age at death. The animals were sacrificed when the mouse was unable to right itself within 30 s when positioned in a supine position (Li et al., 2000).

Tissue Analysis

The animals were sacrificed at the end stage of the disease, perfused, and fixed with 4% paraformaldehyde in PBS (pH 7.4). The spinal cord was isolated, immersed in paraformaldehyde solution for 1 hr followed by 20% sucrose solution in PBS (pH 7.4) overnight, and frozen in Tissue-Tek Optimal Cutting Temperature compound with liquid nitrogen. The tissues were cryosectioned and mounted on gelatinized glass slides. Every tenth section of 20 μm was collected. All sections were blocked with 1% fetal calf serum in PBS and permeabilized with 0.25% Triton X-100. Sections were processed for multiple markers to determine the cellular phenotype of GFP-labeled cells. Primary antibodies were added overnight at 4°C for NEUN (mouse monoclonal, 1:200; Chemicon International), beta III-tubulin (mouse monoclonal, 1:200; Chemicon International), MAP2 (mouse monoclonal, 1:200; Sigma-Aldrich), anti-CHAT (rabbit polyclonal; 1:100 Chemicon International), nestin (1:200, Millipore), oligodendrocyte marker O4 (mouse monoclonal, 1:200; Chemicon), and glial fibrillary acidic protein (GFAP, mouse monoclonal, 1:200; Sigma). Mouse and rabbit antibodies conjugated with R-phycoerythrin, Cyanine-3, or biotin (1:200; Jackson ImmunoResearch Laboratories and Dako) were used for 1 hr at room temperature as secondary antibodies when unconjugated primary antibodies were used. The numerical cell density on fixed sections was estimated using the optical dissector method as described previously (Locatelli et al., 2007; Corti et al., 2008). Optical dissectors sized at 100 × 70 × 14 μm were randomly sampled, and the number of positive cells in each dissector was quantified. The density was calculated by dividing the total number of donor cells by the total volume of optical dissectors. The total volume of tissue per specimen (Vcord) containing donor cells was calculated using the Cavalieri method (Corti et al., 2008). This total volume of tissue, multiplied by the number of donor cells per mm^3 (Nv), gave the total number of donor cells per specimen (n = Nv × Vcord).

Histological Analysis

The lumbar spinal cord region was processed for paraffin embedding. Serial cross sections (12 μm thick) of the lumbar spinal cords were made, and every fifth section was processed and Nissl stained, as reported previously (Grondard et al., 2005). The number and diameter (soma) of all motor neurons counted in these cross sections (n = 50 for each mouse) were analyzed. The sections were analyzed at 200 × magnification in the anterior horn (either left or right) for the presence of all neurons in that region. All cells were counted within the ventral horn below an arbitrary horizontal line drawn from the central canal. Only neuronal cells with at least one nucleolus located within the nucleus were counted, as previously described (Grondard et al., 2005).

The axonal count was performed as previously described on semi-thin transverse sections (1 μm) stained with toluidine blue (Corti et al., 2006). Lumbarra anterior roots were examined for axon counting on the optic microscope.

Coculture of Murine Spinal Primary Motor Neurons and Neural Stem Cells

We derived primary motor neuron cultures from E12.5 *nmd* and WT mice as previously described (Corti et al., 2008). The culture medium was a motor neuron medium supplemented with a cocktail of trophic factors (Corti et al., 2008). We performed a coculture assay to separate the primary motor neurons from the NSCs with a microporous membrane as previously described (Locatelli et al., 2007; Corti et al., 2008). To evaluate whether hNSCs can protect mouse spinal cord motor neurons of *nmd* mice from the neurotoxic effects of activated microglia, mouse microglia were derived as previously described (Xiao et al., 2007) and cultured, and the conditioned medium was collected after 24 hr from control microglia and microglia activated with 100 ng/ml of lipopolysaccharide (LPS) (Sigma). The microglial-conditioned medium was then filtered and used for neuronal survival assays in the presence of hNSCs. For neuron counts, ten fields were randomly chosen for each sample. At least four independent experiments were considered for each condition.

Figure 7. Mechanistic Studies of NSC Coculture Effects on SMARD1 Motor Neurons

(A) NSC coculture promotes the phosphorylation of GSK-3 on the S9 residue, thus inhibiting enzyme activity with respect to untreated cells (n = 5 independent experiments for each condition; *p < 0.01).

(B) Western blot analysis of the phosphorylation of GSK-3 on S9 showing the increased phosphorylation in treated cells relative to untreated samples.

(C) Representative image of immunocytochemistry to detect phosphorylation of the S9 residue of the GSK3 enzyme in the presence (TR-SMARD1) or absence (SMARD1) of NSCs. Motor neurons were stained with Hb9-GFP (green) and p-GSK-S9 (red). Blue, DAPI nuclear stain. Scale bar, 75 μm.

(D) A survival assay using GSK-3 inhibitors VIII and XIII (without coculture of NSCs) resulted in a significant improvement in survival but not as efficacious as that achieved with NSC coculture (upper panel). In a further step, we inhibited PI3K/AKT using LY294002, which induced dose-dependent death of motor neurons (middle panel), and then evaluated the ability of NSCs and GSK-3 inhibitors to attenuate motor neuron death. NSCs were superior to the two GSK-3 inhibitors in protecting motor neurons from the effects of PI3K inhibition. We obtained similar results with PI-103, a stronger and more specific PI3K inhibitor (lower panel) (n = 5 independent experiments for each condition; *p < 0.01).

(E) A schematic representation of the GSK-3 survival pathway that is modulated by NSC coculture. These experiments were performed with iPSC lines of two SMARD1 patients and WT subjects (three clones for each subject).

Coculture of Human SMARD1 Motor Neurons with NSCs

To develop a coculture of NSCs and human motor neurons, we plated iPSC-derived motor neurons on the bottom chamber of a transwell coculture system and cultured them in the presence of human NSCs (Corti et al., 2008, 2012). Only soluble components could diffuse through the porous membrane that separated the two compartments. In coculture experiments for the evaluation of the effect of neurotrophic factors produced from NSCs, we cultured motor neurons in the absence of further addition of growth factors. To identify motor neurons, fixed cultures were stained using antibodies against βIII-tubulin (1:200), ISLET1/2 (1:200), HB9 (1:200), CHAT (1:200; Millipore), mouse anti-microtubule-associated protein 2 (MAP2, 1:100; Sigma), and SMI-32 (Covance, 1:500); in addition, we quantified them using identification of *Hb9*::*GFP*, counting ten randomly selected fields/well (three wells/condition/experiment in four to five experiments). Morphometric axonal length measurement was made using soma diameter and length distance between two points. We analyzed differences in the results (mean ± SEM for five independent experiments) with the Kolmogorov-Smirnov test (http://www.physics.csbsju.edu/stats/KS-test.n.plot_form.html).

Supplemental Experimental Procedures are available online.

SUPPLEMENTAL INFORMATION

Supplemental Information includes Supplemental Experimental Procedures and four figures and can be found with this article online at http://dx.doi.org/10.1016/j.stemcr.2014.06.004.

AUTHOR CONTRIBUTIONS

C.S, M.N., and S.C. performed in vitro and in vivo experiments; F.R. and M.R. performed stem cell in vitro experiments; G.R. participated in neuropathological analysis and assisted with data analysis; S.S. performed proteomic analysis; M.B. participated in vivo experiments; N.B. contributed ideas and supported the work; C.S. M.N., S.C., and G.P.C. conceived the experiments and wrote the manuscript.

ACKNOWLEDGMENTS

We wish to thank the Associazione Amici del Centro Dino Ferrari for their support. The financial support of research grants to S.C. and G.P.C. is gratefully acknowledged: Telethon grant GGP10062 (G.P.C.); Ministry of Health (S.C.): GR-2009-1483560 and GR-2010-2309463, FIRB RBFR08RV86.

Received: February 9, 2014
Revised: June 4, 2014
Accepted: June 5, 2014
Published: July 3, 2014

REFERENCES

Boulis, N.M., Federici, T., Glass, J.D., Lunn, J.S., Sakowski, S.A., and Feldman, E.L. (2011). Translational stem cell therapy for amyotrophic lateral sclerosis. Nat. Rev. Neurol. *8*, 172–176.

Corti, S., Locatelli, F., Papadimitriou, D., Donadoni, C., Del Bo, R., Crimi, M., Bordoni, A., Fortunato, F., Strazzer, S., Menozzi, G., et al. (2006). Transplanted ALDHhiSSClo neural stem cells generate motor neurons and delay disease progression of nmd mice, an animal model of SMARD1. Hum. Mol. Genet. *15*, 167–187.

Corti, S., Nizzardo, M., Nardini, M., Donadoni, C., Salani, S., Ronchi, D., Saladino, F., Bordoni, A., Fortunato, F., Del Bo, R., et al. (2008). Neural stem cell transplantation can ameliorate the phenotype of a mouse model of spinal muscular atrophy. J. Clin. Invest. *118*, 3316–3330.

Corti, S., Nizzardo, M., Nardini, M., Donadoni, C., Salani, S., Del Bo, R., Papadimitriou, D., Locatelli, F., Mezzina, N., Gianni, F., et al. (2009). Motoneuron transplantation rescues the phenotype of SMARD1 (spinal muscular atrophy with respiratory distress type 1). J. Neurosci. *29*, 11761–11771.

Corti, S., Nizzardo, M., Nardini, M., Donadoni, C., Salani, S., Ronchi, D., Simone, C., Falcone, M., Papadimitriou, D., Locatelli, F., et al. (2010). Embryonic stem cell-derived neural stem cells improve spinal muscular atrophy phenotype in mice. Brain *133*, 465–481.

Corti, S., Nizzardo, M., Simone, C., Falcone, M., Nardini, M., Ronchi, D., Donadoni, C., Salani, S., Riboldi, G., Magri, F., et al. (2012). Genetic correction of human induced pluripotent stem cells from patients with spinal muscular atrophy. Sci. Transl. Med. *4*, ra162.

Cox, G.A., Mahaffey, C.L., and Frankel, W.N. (1998). Identification of the mouse neuromuscular degeneration gene and mapping of a second site suppressor allele. Neuron *21*, 1327–1337.

Donnelly, E.M., Lamanna, J., and Boulis, N.M. (2012). Stem cell therapy for the spinal cord. Stem Cell Res. Ther. *3*, 24.

Eckart, M., Guenther, U.P., Idkowiak, J., Varon, R., Grolle, B., Boffi, P., Van Maldergem, L., Hübner, C., Schuelke, M., and von Au, K. (2012). The natural course of infantile spinal muscular atrophy with respiratory distress type 1 (SMARD1). Pediatrics *129*, e148–e156.

Grohmann, K., Schuelke, M., Diers, A., Hoffmann, K., Lucke, B., Adams, C., Bertini, E., Leonhardt-Horti, H., Muntoni, F., Ouvrier, R., et al. (2001). Mutations in the gene encoding immunoglobulin mu-binding protein 2 cause spinal muscular atrophy with respiratory distress type 1. Nat. Genet. *29*, 75–77.

Grondard, C., Biondi, O., Armand, A.S., Lécolle, S., Della Gaspera, B., Pariset, C., Li, H., Gallien, C.L., Vidal, P.P., Chanoine, C., and Charbonnier, F. (2005). Regular exercise prolongs survival in a type 2 spinal muscular atrophy model mouse. J. Neurosci. *25*, 7615–7622.

Guenther, U.P., Handoko, L., Laggerbauer, B., Jablonka, S., Chari, A., Alzheimer, M., Ohmer, J., Plöttner, O., Gehring, N., Sickmann, A., et al. (2009). IGHMBP2 is a ribosome-associated helicase inactive in the neuromuscular disorder distal SMA type 1 (DSMA1). Hum. Mol. Genet. *18*, 1288–1300.

Herdegen, T., Skene, P., and Bähr, M. (1997). The c-Jun transcription factor—bipotential mediator of neuronal death, survival and regeneration. Trends Neurosci. *20*, 227–231.

Hu, B.Y., and Zhang, S.C. (2009). Differentiation of spinal motor neurons from pluripotent human stem cells. Nat. Protoc. *4*, 1295–1304.

Ito, D., Okano, H., and Suzuki, N. (2012). Accelerating progress in induced pluripotent stem cell research for neurological diseases. Ann. Neurol. *72*, 167–174.

Jankowsky, A., Guenther, U.P., and Jankowsky, E. (2011). The RNA helicase database. Nucleic Acids Res. *39*, D338–D341.

Li, Y., Chopp, M., Chen, J., Wang, L., Gautam, S.C., Xu, Y.X., and Zhang, Z. (2000). Intrastriatal transplantation of bone marrow nonhematopoietic cells improves functional recovery after stroke in adult mice. J. Cereb. Blood Flow Metab. *20*, 1311–1319.

Locatelli, F., Corti, S., Papadimitriou, D., Fortunato, F., Del Bo, R., Donadoni, C., Nizzardo, M., Nardini, M., Salani, S., Ghezzi, S., et al. (2007). Fas small interfering RNA reduces motoneuron death in amyotrophic lateral sclerosis mice. Ann. Neurol. *62*, 81–92.

Marchetto, M.C., Muotri, A.R., Mu, Y., Smith, A.M., Cezar, G.G., and Gage, F.H. (2008). Non-cell-autonomous effect of human SOD1 G37R astrocytes on motor neurons derived from human embryonic stem cells. Cell Stem Cell *3*, 649–657.

Nizzardo, M., Simone, C., Rizzo, F., Ruggieri, M., Salani, S., Riboldi, G., Faravelli, I., Zanetta, C., Bresolin, N., Comi, G.P., and Corti, S. (2013). Minimally invasive transplantation of iPSC-derived ALDHhiSSCloVLA4+ neural stem cells effectively improves the phenotype of an amyotrophic lateral sclerosis model. Hum. Mol. Genet.

Teng, Y.D., Benn, S.C., Kalkanis, S.N., Shefner, J.M., Onario, R.C., Cheng, B., Lachyankar, M.B., Marconi, M., Li, J., Yu, D., et al. (2012). Multimodal actions of neural stem cells in a mouse model of ALS: a meta-analysis. Sci. Transl. Med. *4*, ra164.

Xiao, Q., Zhao, W., Beers, D.R., Yen, A.A., Xie, W., Henkel, J.S., and Appel, S.H. (2007). Mutant SOD1(G93A) microglia are more neurotoxic relative to wild-type microglia. J. Neurochem. *102*, 2008–2019.

Yang, Y.M., Gupta, S.K., Kim, K.J., Powers, B.E., Cerqueira, A., Wainger, B.J., Ngo, H.D., Rosowski, K.A., Schein, P.A., Ackeifi, C.A., et al. (2013). A small molecule screen in stem-cell-derived motor neurons identifies a kinase inhibitor as a candidate therapeutic for ALS. Cell Stem Cell *12*, 713–726.

Yu, J., Hu, K., Smuga-Otto, K., Tian, S., Stewart, R., Slukvin, I.I., and Thomson, J.A. (2009). Human induced pluripotent stem cells free of vector and transgene sequences. Science *8*, 797–801.

Zuo, T., Qin, J.Y., Chen, J., Shi, Z., Liu, M., Gao, X., and Gao, D. (2013). Involvement of N-cadherin in the protective effect of glial cell line-derived neurotrophic factor on dopaminergic neuron damage. Int. J. Mol. Med. *31*, 561–568.